SOUTHERN OCEAN FRONTS IN THE BLUELINK REANALYSIS

By Clothilde Langlais[1,2] , Andreas Schiller[2,3], Peter R. Oke[2,3]

[1]University of Tasmania, Sandy Bay TAS, Australia
[2]Commonwealth Scientific and Industrial Research Organisation Wealth from Oceans National Research Flagship, Hobart, Australia
[3] CAWCR-CSIRO, Castray Esplanade 7000 Hobart TAS, Australia

Introduction

The Southern Ocean (SO) has a central place in the global thermohaline circulation. Most of the major water masses of the global ocean cross each other around Antarctica, being upwelled, transformed, subducted or simply generated in the area. The meridional overturning circulation of the water masses induces a southward shoaling of the isotherms that is associated with the Antarctic Circumpolar Current (ACC). The ACC consists in several circumpolar jets or fronts that separate different geographic zones with distinct physical and bio-chemical properties.

A variety of definitions have been used to identify the fronts of the Southern Ocean. Arising from hydrographic cruises, the definitions are usually based on criteria related to the interior ocean structure: transport maxima, gradients along particular isopycnals, latitude where a property isoline crosses a particular isobar (Peterson and Stramma, 1991; Orsi et al. 1995 ; Belkin and Gordon, 1996 ; Sokolov and Rintoul, 2002). The same simple phenomenological criteria can be used to locate the fronts along their circumpolar extent. Those definitions underline the persistent and robust character of the fronts.

High resolution observations (satellite altimetry, high resolution hydrographic sections) and numerical models have revealed more complex structures than the climatological hydrographic data, with multiple branches that merge and diverge (Sinha and Richards, 1999; Hughes and Ash, 2001, Sokolov and Rintoul, 2008). From those observations, new frontal definitions appeared. As the ACC is associated with large geostrophic currents, the fronts can be associated with sea surface temperature (SST) and sea surface height (SSH) gradients (Gille, 1994; Hughes and Ash, 2001; Dong H et al. 2006 ; Sokolov and Rintoul, 2008).

More recently, Sokolov and Rintoul (2008) showed that each ACC branch remains mainly associated with a particular streamline. The association between jets and streamlines appears to be persistent along the circumpolar pathway despite the interactions with bathymetry and eddies. In equivalent barotropic flow like in the SO, the streamlines can be approximated by SSH contours (Killworth and Hughes, 2002). Particular values of SSH can then be used to define fronts in the SO: a maximum in SSH gradient (the core of a ACC jet) can be tracked with a particular SSH contour. By applying a nonlinear fitting procedure, Sokolov and Rintoul (2008) identified ten SSH values that describe the multi-branch structure of the ACC south of Australia (100 to 180 ºE) during a 12 year period.

In equivalent-barotropic flow, the streamlines correspond to a particular water column structure (Sun and Watts, 2001; Watts et al. 2001).This means that frontal definitions based on either SSH values or on water mass properties should give the same frontal positions in such a flow regime. This idea is confirmed in Sallee et al. (2008) where the frontal SSH contours are found by using subsurface hydrography.

In this paper, we combine hydrologic and dynamic criteria to identify the ACC fronts in the Bluelink ocean model, including a free run and an assimilating run. Our objective is to reveal the time and spatial variability of the fronts. We apply a SSH contour criteria to define the ACC fronts from Ocean General Circulation Model (OGCM) outputs. To identify the SSH contours, we use the SO thermodynamical structure, i.e. water masses and transport properties.

After a description of the model runs, the method used to identify the ACC fronts is described. The variability of the fronts in the SO is then presented, followed by our conclusions.

Ocean model and assimilation

The OGCM is based on version 4p1 of the Modular Ocean Model (Griffies, 2004) with a free surface formulation. No horizontal diffusion is applied and the horizontal viscosity is resolution and state-dependent based on the Smagorinsky scheme with a biharmonic operator (Griffies and Hallberg, 2000). For tracer advection, the model uses the third-order quicker scheme (Leonard, 1979). For vertical mixing, the hybrid mixed layer model described by Chen et al. (1994) is used: under a Niiler-Klaus bulk layer, the mixing is parametrized with a Richardson number dependent scheme.

The model configuration is called Ocean Forecasting Australia Model (OFAM) with a resolution of 1/10° in the Asian-Australian region (90-180°E, south of 17°). Outside this domain, the horizontal resolution decreases to 1o across the Indian and Pacific Oceans and 2° in the Atlantic Ocean. OFAM has 47 vertical levels, with 10 m resolution to 200m depth and 35 levels in the top 1000m. Partial cells are used at the bottom.

The Bluelink ReANalysis (BRAN; Schiller et al. 2008) is a multiyear model run with data assimilation. Observations assimilated in BRAN includes sea-level anomaly (SLA) from satelllite altimetry and tide gauges, satellite-derived SST and in situ Temperature (T) and Salinity profiles (Argo floats, CTD, XBT, TAO array...). The Bluelink Ocean Data Assimilation System (BODAS) is an ensemble optimal interpolation system (Oke et al. 2008). In order to project the observations onto the full ocean model state, BODAS uses model-based, multivariate background error covariances. BODAS is used to sequentially assimilate observations once every 7 days.

BRAN is integrated from 1992 to 2006 and forced with interannual 6-hourly surface fluxes. From 1992 to mid-2002, wind stress, heat and freshwater fluxes are provided by the ERA40 reanalysis (Kallberg et al., 2004) and from mid-2002 until 2006 by the ECMWF forecast. The initial conditions come from a 13 years spin-up run, spanning 1994-2002, with no data assimilation. The spin-up run is initialized with a blend of CARS climatologies (CSIRO Atlas of Regional Seas; Ridgway et al., 2002) and Levitus (1989). During the first year of integration of the spin-up run, OFAM is forced with climatological surface fluxes (Southampton Oceanographic Centre, Josey et al., 1998). Forcing fields are provided by the ERA40 reanalysis for the period 1994-2006, with restoring surface salinity to Levitus (2001) over a 30 day period.

For this study, fields from BRAN and the spin-up run, hereafter referred to as the OFAM free run, are used as databases to identify the ACC fronts.

ACC Fronts

Transport and temperature criteria as front indicators

A natural definition of a front in the SO is the maximum of gradients of SSH or SST. Since the OGCM provides a complete description of the ocean circulation, we can explore characteristics of fronts by examining many aspects of the time-evolving temperature, salinity, and density, as well as zonal total transport and geostrophic transport, for all meridional sections south of Australia. Figure 1 presents meridional sections of temperature and zonal transport at 135ºE for the two databases used here in January 1998. The model simulations reveal a complex structure of the SO with multiple ACC fronts, meanders and eddies.

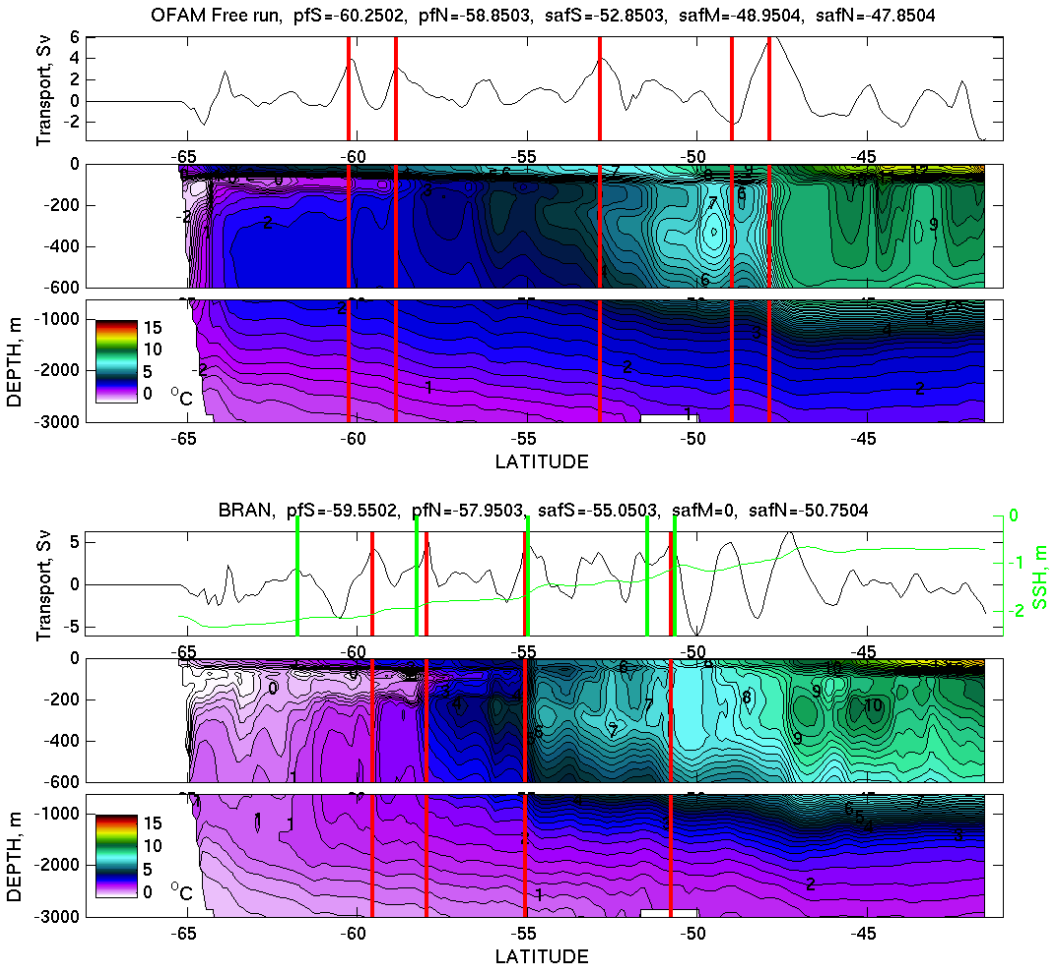

Figure 1

Transport (Sv) and temperature (°C) at 135ºE section along with fronts positions using the transport and Temperature criteria in red and using the SSH criteria in green for January 1998. Upper panels: OFAM free run, lower panels: BRAN.

Consistent with previous findings (Belkin and Gordon, 1996; Sokolov and Rintoul, 2002), the Subantarctic Front (SAF) corresponds to maxima of transport and maxima of temperature gradient between 300 and 400 m. The northern Polar Front (PF-N) is the northern limit of the Antarctic zone and a traditional limit is the northern extent of the Antarctic Winter Water (AAWW) characterized by subsurface temperature minima. In the two simulations (OFAM and BRAN), the northern end of the subsurface temperature minimum layer (Tmin-layer) is associated with a maximum of transport and a maximum of gradient along the Tmin-layer. The southern Polar Front (PF-S) coincides with an increase in depth of the Tmin-layer (Gordon, 1967, 1971) and an enhanced temperature gradient along the Tmin-layer (Sokolov and Rintoul, 2002) which leads to a maximum of transport.

However the water masses do not have the same characteristics in the two simulations and the ACC jets are not associated with the same hydrographic limits. Table 1 regroups the temperature criteria used to identify the fronts and compares them with the criteria identified by Sokolov and Rintoul (2002) in the South Australia sector. To identify those limits, we studied the T gradients of interannual means in Tmin-layer and at around 380 m (see table 1 for the exact depth used for the two simulations) for different sections south of Australia (OFAM and BRAN) (see Figure 2 for BRAN). The maxima of the T gradients correspond to the position of the SAF and PF. The fronts are not located at the same latitude all around Antarctica (Figure 2a), but they always occur in particular temperature limits (Figure 2b). Depending on the longitude, we can identify two or three SAFs.

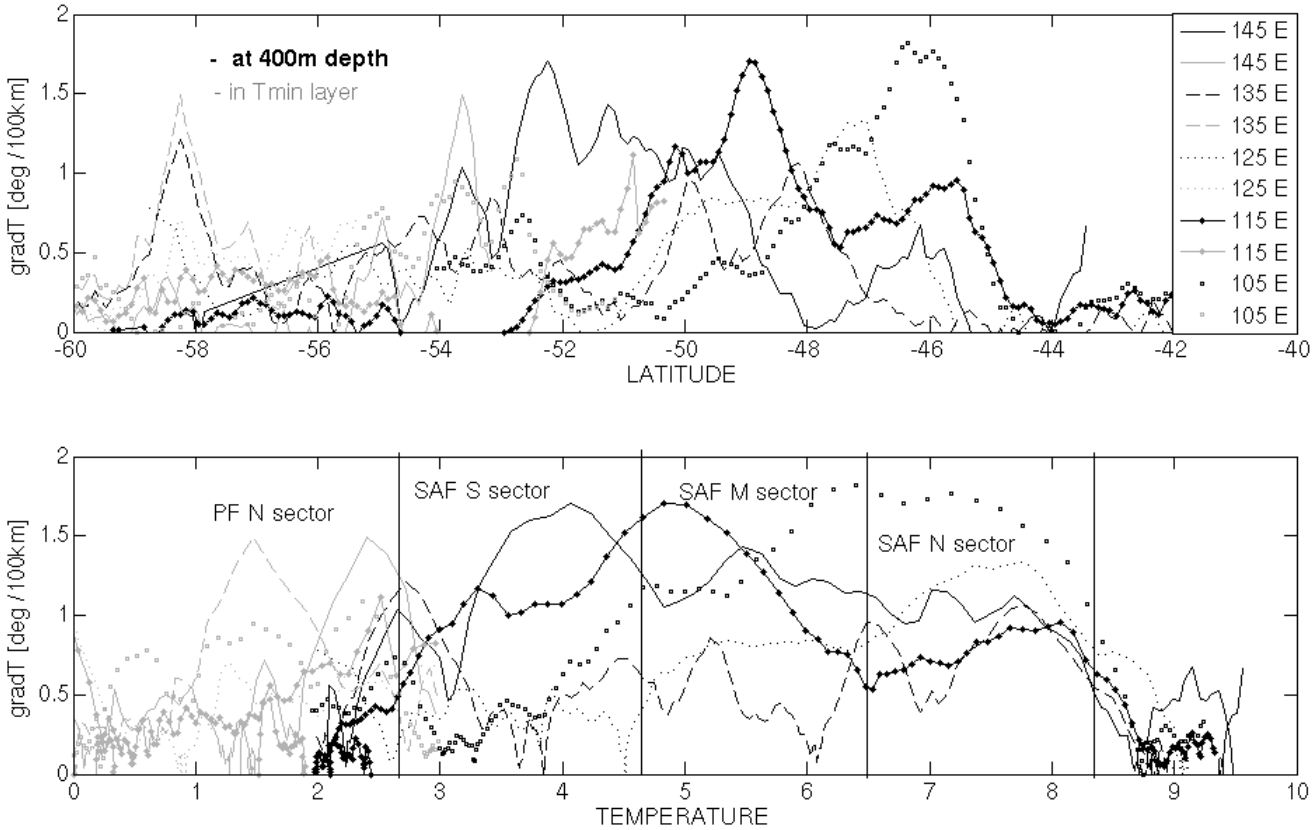

Figure 2

BRAN meridional temperature gradients (°C/100km) in the subsurface temperature minimum layer (grey lines) and at 372m depth (black lines) for different longitude south of Australia (top) as a function of latitude, and (bottom) as a function of temperature.

Fronts		OFAM	BRAN	Sokolov and Rintoul, 2002
SAFs	depth/level	372 m / level 28	372 m / level 28	400 dbar
SAFs	Transport maxima between	3ºC < T < 9ºC	3ºC < T < 8.5ºC	
SAF-N	T limits	7ºC < T < 8.75ºC	6.5ºC < T < 8.25ºC	6ºC < T < 8ºC
SAF-M	T limits	5ºC < T < 7ºC	4.7ºC < T < 6.5ºC	5ºC < T < 6ºC
SAF-S	T limits	3ºC < T < 5ºC	2.6ºC < T < 4.7ºC	4ºC < T < 5ºC
PF	T limit of AAWW	3.2ºC	2.8ºC	2ºC

Table 1

Front indicators for the two simulations, OFAM and BRAN, and comparison with the indicators for the Australian sector of the Southern Ocean from Sokolov and Rintoul (2002).

The identification of the three SAFs and two PFs is performed on weekly mean outputs for all the meridional sections south of Australia. To locate the SAF on meridional sections, we first identify the position of the transport maxima within an area delimited by T characteristics around 380 m depth. Each transport maxima is then associated with a particular front regarding the T characteristic around 380 m. For the PF-N, we monitor the AAWW, following the depth and temperature of the Tmin-layer. We use the T limit of table 1 to identify the northern limit of the AAWW. The PF-N is then defined as the maximum of transport south of this limit. For the PF-S, we locate the maximum of increase in depth of the Tmin-layer. The PF-S corresponds to the maximum of transport nearby this position. The results for the 135ºE section are shown on Figure 1.

Towards SSH contours

Using transport and temperature criteria has the advantage to reconcile two frontal views: the hydrographic and dynamical views. The traditional hydrographic indicators underline the persistence of the fronts that separate different bio-geo-hydrographic zones. The maximum of transport criteria ensures that our analysis also reflects the dynamical part of the fronts that are associated with large geostrophic currents, the ACC jets.

However the method has some limitations. Since we identify the fronts on weekly mean outputs, meanders and eddies perturb the transport and temperature fields, thereby complicating the identification of the fronts. The merging and splitting of the fronts can limit the number of fronts. Large meandering or deflection of the fronts can lead to two meridional positions for one single front.

The seasonal formation of a summer thermocline is also problematic for the study of the Tmin-layer. Since the AAWW are generated during the winter, the Tmin-layer is a subsurface layer in summer but reach the surface in winter. Our transport and temperature criteria for the southern front tend to identify the PF-S during the summer and the South ACC front (sACCf) in winter.

Another limitation comes from the temperature limits (table 1). Frequency distributions of temperature for the ACC fronts do not reveal a particular isotherm but exhibit broad Gaussian variations that overlap (figure not shown). As a result, a particular isotherm may correspond to two different fronts that our method cannot reliably distinguish between. Figure 3 underlines this tendency to jump from one front to another.

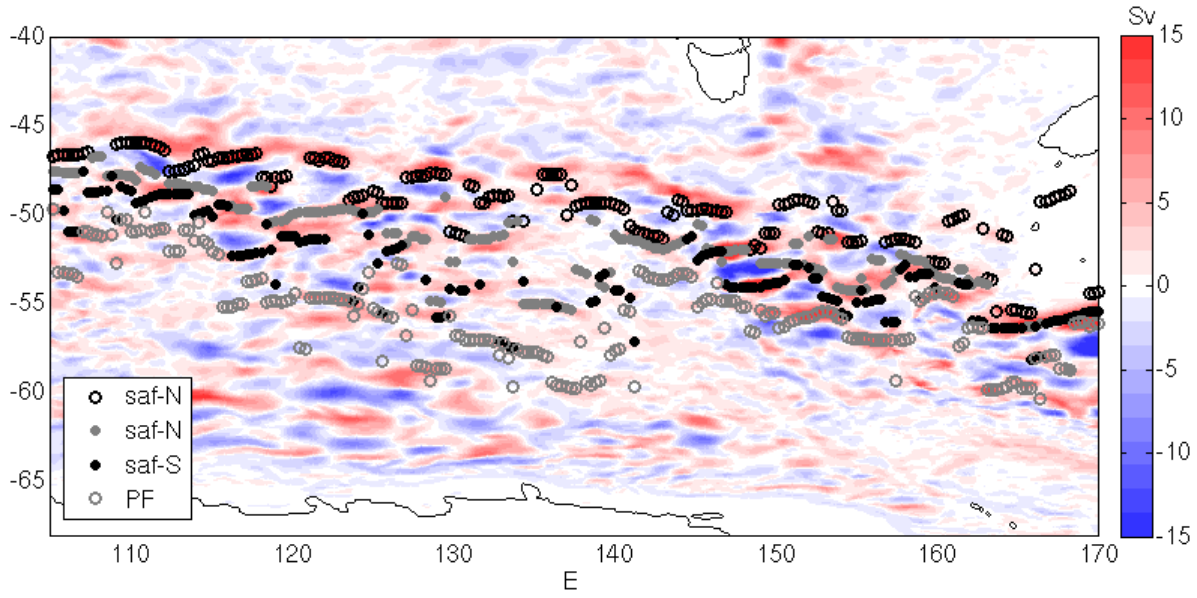

Figure 3
Transport field (Sv, red and blue colors) south of Australia (week 8 1998) overlaid with the position of the 4 ACC fronts (black and grey) identified with the transport and temperature criteria for BRAN.

The results obtained with the transport and temperature criteria are used as a first guess to locate five of the main ACC jets. Using frequency distribution of SSH for this frontal database, we then identify SSH contours that best fit each front. Figure 4 shows histograms of the SSH contours derived from this weekly database for BRAN. Because of uncertainty distinguishing different fronts using transport and temperature criteria, the Gaussian peaks of the histogram overlap. However, as mentioned by Sokolov and Rintoul (2008) and Sallee et al. (2008), each front is characterized by a particular SSH value.

Table 2 regroups the SSH contour values for BRAN. Unfortunately, the SSH contour definition can not be applied to OFAM because of long-term SSH trends that are present in the simulation.

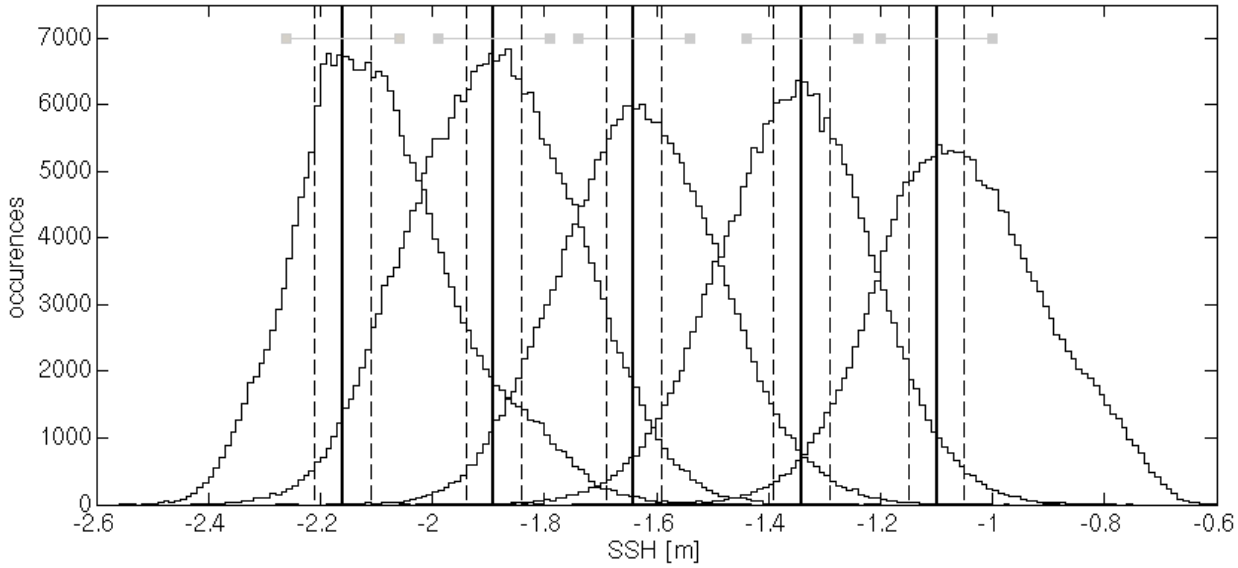

Figure 4
Frequency distribution of SSH contours (number of occurences) for the fronts identified with the transport and temperature criteria method for BRAN. The vertical lines identify some windows around the peak value for the SSH filtering.

Fronts	BRAN
SAF-N	-1.1
SAF-M	-1.34
SAF-S	-1.64
PF	-1.89
sACCf	-2.16

Table 2
SSH contour values (m) associated with the ACC fronts in the Southern Ocean for the BRAN reanalysis (South Australian sector).

Reanalysis (BRAN) versus Non-Assimilating Model (OFAM)

Because of assimilation, one can argue that the jets in BRAN are controlled by altimetry and do not represent hydro-geographic barriers that separate the water masses in the SO. A comparison between BRAN and OFAM is necessary to ensure that the fronts identified in BRAN are due to the model physics and not the assimilation step.

Our method based on transport and temperature criteria does not reliably distinguish the fronts (figure 3). To remove the uncertainty and identify a single front, the best-fit SSH contours are used as filter value.. A window of +/- 0.1 m around the SSH peak values (figure 4) is applied to filter the database of frontal positions. Figure 5 shows the mean position of the ACC fronts in the Australian sector for the two simulations. The mean PF-S and SAF-N positions from Sallee et al. (2008) and the mean fronts from Sokolov and Rintoul (2008) are also superimposed. The fronts of the two model runs exhibit similar spatial patterns, with the same meandering tendency downstream of the main bathymetric features. Their positions agree quite well, especially when the fronts are steered by the fractures of the southeast Indian Ridge or by the Campbell Plateau, and when they cross the Macquarie Ridge. If our SAF agree globally with the mean SAF position of Sokolov and Rintoul (2008) and Sallee et al. (2008), our PF seems to differ as our PF-N seems to correspond to their PF-S and our PF-S more likely corresponds to a South ACC front (sACCf). The Tmin-layer approach is problematic in winter, when the surface mixed-layer is deep. By contrast, the SSH filtering approach can identify a single front in both winter and summer.

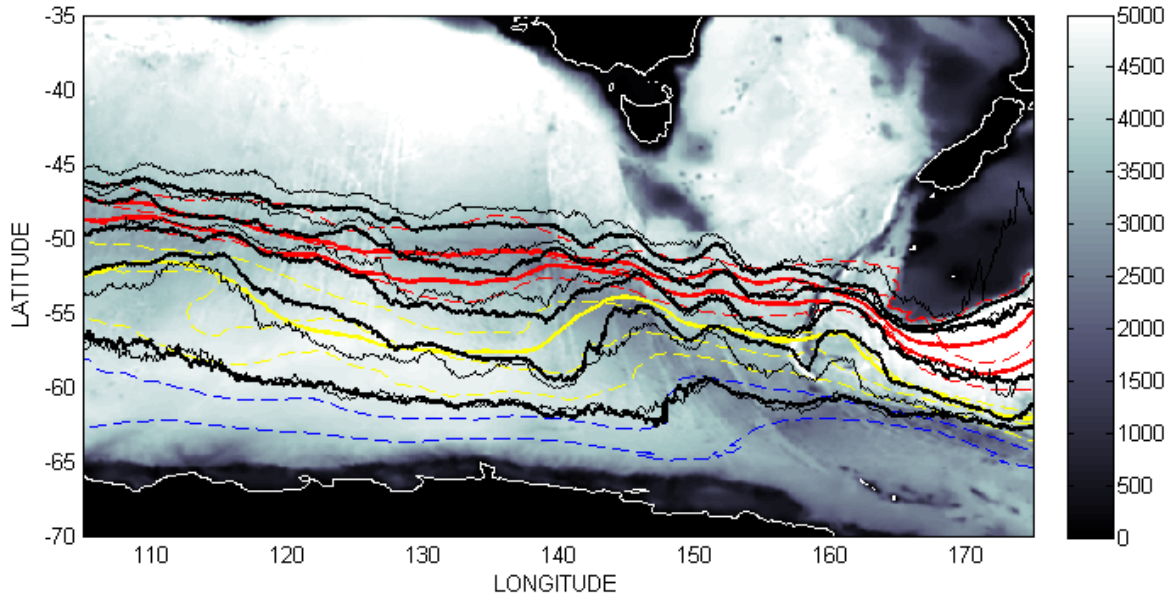

Figure 5

Mean ACC fronts position from the transport and temperature criteria with a SSH filtering for OFAM (black) and BRAN (thick black) superimposed with the bathymetry (m) in the south Australian sector. The ACC fronts from Sallee et al., (2008) (color dash lines) and from Sokolov and Rintoul (2008) (color lines) are also represented: SAF in red, PF in yellow and sACCf in blue.

SSH contours versus hydro-dynamic criteria

In figure 1, the frontal positions of the transport and temperature method and of the SSH contour method can be analyzed and compared for a section south of Australia. The sections and dates chosen for figure 1 underline the main agreements and discrepancies found all around Antarctica. For the SAF and PF, the two methods give similar positions which are superimposed most of the time, with discrepancies of no more than 0.5°C (figure 1). For the position of the sACCf, the discrepancy between the two methods is more significant and can reach a few degrees. In summer, the southern front corresponds to the PF-N for the transport and temperature criteria and to the sACCf for the SSH contour definition. The SSH contours method has the advantage of revealing the five fronts systematically.

In figure 6, the SSH contours fronts follow and join the strongest simulated ACC jet. The SAF-N and M appear to be the most intense current jets south of Australia (figure 6).

Figures 1 and 6 confirm that SSH contours can be used to approximate streamlines (in particular the core of the ACC jets) and can be associated with subsurface hydrographic structure in the Southern Ocean.

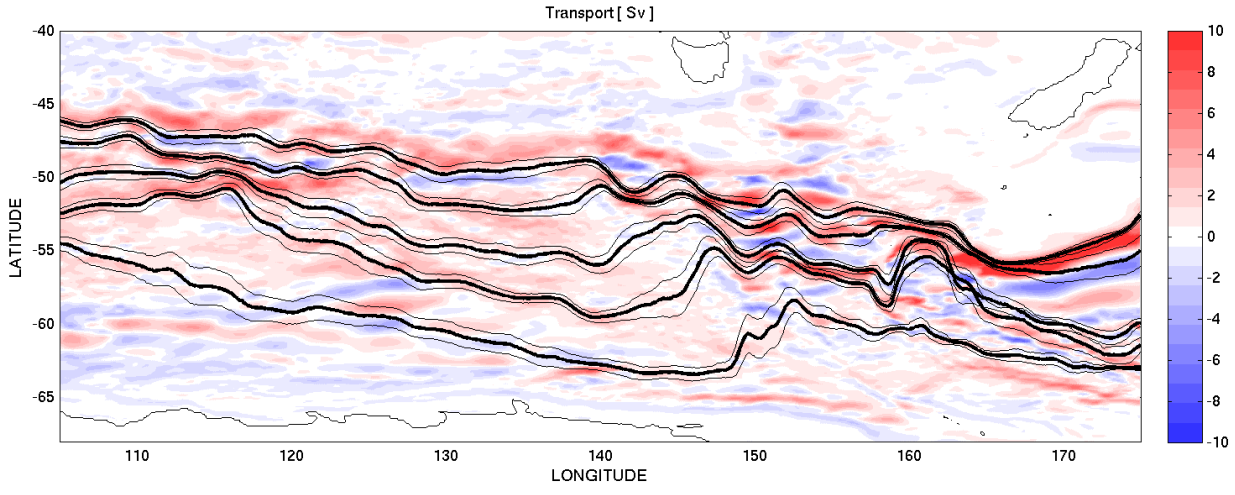

Figure 6

Mean SSH gradient (Sv, read and blue colors) superimposed with the mean positions of fronts for BRAN (bold black lines). The standard deviation envelope (meridional spatial variability) of the fronts position is represented by thin black lines.

Variability of the ACC fronts

ACC fronts mean positions

The mean frontal positions of BRAN agree quite well with the mean positions of Sallee et al., (2008) and Sokolov and Rintoul (2008) (figure 5). In both cases, mean pathways and meridional deflections of the fronts are controlled by topography. Along its circumpolar path, the ACC has a number of large topographic barriers that perturb the flow. South of Australia, the main obstacles are the South-eastern Indian Ridges, the South Tasmanian Ridge (SIR), the Macquarie Ridge and the Campbell Plateau. The ACC fronts are typically steered around these obstacles or over the shallow plateau. The topographic steering leads to sharp meridional deflection. When a jet is constrained to pass over a shallow plateau or ridge, all the fronts tend to move equatorward to compensate for loss of potential vorticity.

Downstream of topographic barriers, mesoscale activity tends to be developed. The frontal meandering is coherent and persistent enough to appear in the mean position of the fronts. Those coherent mesoscale meanders are less clear in the frontal database calculated from satellite altimetry products than in BRAN. South of the SIR (downstream of the SIR), two meanders are very distinct. A weaker signature of those meanders can be observed in Sallee et al., (2008) but do not appear in Sokolov and Rintoul (2008). Downstream of the Macquarie Ridge, all the fronts deflect northward and are then constrain to deflect southward by the Campbell Plateau, generating sharp meanders with an amplitude of almost 4°. Once again this signature is not clearly revealed in Sallee et al., (2008) or Sokolov and Rintoul (2008).

Variability

The topography not only controls the pathways of the ACC fronts but also their variability (e.g., Gordon et al. 1978; Chelton et al. 1990; Gille 1994; Moore et al. 1999; Sokolov and Rintoul 2008; Dong et al. 2006). Steep bottom slopes are associated with very weak variations of the front position, whereas flat-bottom areas are subject to large movement of the fronts (Figure 6). When the jets are steered by topography, the meridional variability drops and the intensity of the flow increases. When the fronts cross a shallow plateau or ridge, a drop of variability is also observed and is associated with a decrease in the intensity of the jets. Over the abyssal plain, the intensity of the fronts stays quite strong with an increase in variability. With no bathymetric control, the fronts are predominantly forced by atmospheric forcing and the meridional movements of fronts can be correlated with climatic modes from ENSO (El Nino Southern Oscillation) and SAM (Southern Annular Mode) (Sallee et al, 2008).

Conclusion

A SSH contours are found by using subsurface hydrography combined with depth integrated properties. The results for the reanalysis and from a free model run are quite consistent, giving us confidence in BRAN fronts positions database. The positions of the fronts are controlled primarily by the model physics and not by the assimilation step.

The next step is to use this ACC fronts analysis as a tool to perform intercomparisons with the next generation of BRAN and OFAM runs, and also intercomparisons with other reanalysis (e.g., GLORYS) or OGCM (ORCA025, Langlais et al., 2010). This new metric will enhance our understanding of the differences between the hydrographic definitions of the fronts and the differences in the spatial position and variability of the ACC jets.

Acknowledgements

Financial support for this research is provided by the Quantitative Marine Science joint program between University of Tasmania and CSIRO and through the CSIRO Wealth from Ocean flagship program.

References

Belkin, I. M., and A. L. Gordon, 1996: Southern Ocean fronts from the Greenwich Meridian to Tasmania. *J. Geophys. Res.*, **101**, 3675-3696.

Chelton, D.B., M.G. Schlax, D.L. Witter, and J.G. Richman, 1990: Geosat Altimeter Observations of the Surface Circulation of the Southern Ocean, *J. Geophys. Res.*, **95**(C 10), 17877-17903.

Chen, D., L.Rothstein, and A.Busalacchi, 1994: A hybrid vertical mixing scheme and its application to tropical ocean models, *Journal of Physical Oceanography*, **24**, 2156-2179.

Dong, S., J. Sprintall, and S. T. Gille, 2006: Location of the Antarctic polar front from AMSR-E satellite sea surface temperature measurements. *J. Phys. Oceanogr.*, **36**, 2075-2089.

Gille, S. T., 1994: Mean sea surface height of the Antarctic Circumpolar Current from Geosat data: Method and application. *J. Geophys. Res.*, **99**, 18 255-18 273.

Gordon, A.L., 1967. Structure of Antarctic waters between 20°W and 170°W. Am. Geogr. Soc. Antarct. Map Folio Ser., Folio 6 (10 pp.).

Gordon, A.L., 1971. The Antarctic Polar Front zone. In: Reid, 1096 J.L. (Ed.), Antarctic Oceanology I. Antarctic Research Series, 1097 vol. 15. American Geophysical Union, pp. 205-221.

Gordon, A. L., E. Molinelli, and T. Baker, 1978: Large-scale relative topography of the Southern Ocean. *J. Geophys. Res.*, **83**, 3023-3032.

Griffies, S.M., 2004: Fundamentals of ocean climate models, Princeton University Press, Princeton, USA,

Griffies, S.M., and R.W. Hallberg, 2000: Biharmonic friction with a Smagorinsky viscosity for use in large-scale eddypermitting ocean models, *Monthly Weather Review*, **128**, 2935-2946.

Hughes, C. W., and E. Ash, 2001: Eddy forcing of the mean flow in the Southern Ocean. *J. Geophys. Res.*, **106**, 2713-2722.

Josey, S.A., Kent, E.C., Taylor, P.K., 1998. The Southsampton Pceanography Centre (SOC) ocen-atmosphere heat, momentum and freshwater flux atlas. Southampton Oceanography Centre, report No. 6, 30 pp.

Kallberg, P., A. Simmons, S. Uppala, M. Fuentes (2004), The ERA-40 Archive, ERA-40 Project Report Series No. 17, ECMWF.

Killworth, P. D., and C. W. Hughes, 2002: The Antarctic Circumpolar Current as a free equivalent-barotropic jet. *J. Mar. Res.*, **60**, 19-45.

Langlais C., Schiller A., Rintoul S., Coleman R. 2010 : Variability of the Southern Ocean fronts. In preparation.

Leonard, B. P., 1979: A stable and accurate convective modeling procedure based on quadratic upstream interpolation. *Comput. Methods Appl. Mech. Eng.*, **19**, 59-98

Levitus, S. , 1989: Interpentadal variability of temperature and salinity in the deep North Atlantic, 1970 - 74 versus 1955 - 59, *J. Geophys. Res.*, **94**, 16,125 - 16,131.

Levitus S., 2001. World Ocean Database, vol. 13. U.S. Department of Commerce. National Oceanic and Atmospheric Administration.

Moore, J., M. Abbott, and J. Richman, 1999: Location and dynamics of the Antarctic polar front from Satellite Sea surface temperature data. *J. Geophys. Res.*, **104**, 3059-3073.

Oke, P. R., G. B. Brassington, D. A. Griffin and A. Schiller, 2008: The Bluelink Ocean Data Assimilation System (BODAS), *Ocean Modelling*, **21**, 46-70

Orsi, A., T. Whitworth III, and W. Nowlin Jr., 1995: On the meridional extent and fronts of the Antarctic Circumpolar Current. *Deep-Sea Res. II*, **42**, 641-673.

Peterson, R. G., and L. Stramma, 1991: Upper-level circulation in the South Atlantic Ocean. *Prog. Oceanogr.*, **26**, 1-73.

Ridgway, K. R., J. R. Dunn, and J. L. Wilkin, 2002 : Ocean Interpolation by Four-Dimensional Weighted Least Squares-Application to the Waters around Australasia, *Journal of atmospheric and oceanic technology*, **19**, 1357-1374

Sallee, J.B., K. Speer, and R. Morrow, 2008: Response of the Antarctic Circumpolar Current to Atmospheric Variability, *Journal of Climate*, **21**, 3020-3039.

Schiller, A., P. R. Oke, G. B. Brassington, M. Entel, R. Fiedler, D. A. Griffin, and J. V. Mansbridge, 2008: Eddy-resolving ocean circulation in the Asian-Australian region inferred from an ocean reanalysis effort. *Progress in Oceanography*, **76**, 334-365.

Sinha, B., and K. J. Richards, 1999: Jet structure and scaling in Southern Ocean models. *J. Phys. Oceanogr.*, **29**, 1143-1155.

Sokolov, S., and S. R. Rintoul, 2002: Structure of Southern Ocean fronts at 140°E. *J. Mar. Syst.*, **37**, 151-184.

Sokolov, S., and S. R. Rintoul 2007 or 2008?: Multiple jets of the Antarctic Circumpolar Current south of Australia. *J. Phys. Oceanogr.*, **37**, 1394-1412.

Sun, C., and D. R. Watts, 2001: A circumpolar gravest empirical mode for the Southern Ocean hydrography. *J. Geophys. Res.*, **106**, 2833-2856.

Watts, D. R., C. Sun, and S. R. Rintoul, 2001: A two-dimentional gravest empirical modes determined from hydrographic observations in the Subantarctic Front. *J. Phys. Oceanogr.*, **31**, 2186-2209.